



UNIVERSITY
OF WOLLONGONG
AUSTRALIA

University of Wollongong
Research Online

Faculty of Engineering and Information Sciences -
Papers: Part A

Faculty of Engineering and Information Sciences

2008

Implementing analytical geometric and penetration response correction for keel-edge pinhole SPECT image reconstruction

Xuezhu Zhang

Chinese Academy Of Sciences

Qiusheng Dai

Chinese Academy Of Sciences

Yujin Qi

Chinese Academy Of Sciences, yujin@uow.edu.au

Publication Details

Zhang, X., Dai, Q. & Qi, Y. (2008). Implementing analytical geometric and penetration response correction for keel-edge pinhole SPECT image reconstruction. 2008 IEEE Nuclear Science Symposium Conference Record (pp. 5255-5259). USA: IEEE.

Research Online is the open access institutional repository for the University of Wollongong. For further information contact the UOW Library:
research-pubs@uow.edu.au

Implementing analytical geometric and penetration response correction for keel-edge pinhole SPECT image reconstruction

Abstract

The collimator response compensation is very important in high-resolution pinhole SPECT imaging for resolution recovery and quantitative imaging. In this study the pinhole collimator response of the keel-edge aperture was investigated in terms of the geometric response function and penetration response function (GPRF). An approximate numerical method was proposed to implement the geometric and penetration response correction (GPRC) for keel-edge pinhole SPECT image reconstruction. A lookup table for the GPRC was calculated and then was utilized in the 3D pinhole iterative OSEM reconstruction procedure. The performance of the image reconstruction with the GPRC was evaluated using both the phantom and small-animal experiments in our micro-SPECT system. The results demonstrated significant improvements in the reconstructed image quality and resolution recovery. In conclusion, our approach using the GPRC method to the resolution recovery for the pinhole SPECT imaging is effective.

Keywords

spect, keel, image, reconstruction, correction, edge, pinhole, response, penetration, geometric, analytical, implementing

Disciplines

Engineering | Science and Technology Studies

Publication Details

Zhang, X., Dai, Q. & Qi, Y. (2008). Implementing analytical geometric and penetration response correction for keel-edge pinhole SPECT image reconstruction. 2008 IEEE Nuclear Science Symposium Conference Record (pp. 5255-5259). USA: IEEE.

Implementing Analytical Geometric and Penetration Response Correction for Keel-edge Pinhole SPECT Image Reconstruction

Xuezhu Zhang, *Student Member, IEEE*, Qiusheng Dai, and Yujin Qi, *Member, IEEE*

Abstract—The collimator response compensation is very important in high-resolution pinhole SPECT imaging for resolution recovery and quantitative imaging. In this study the pinhole collimator response of the keel-edge aperture was investigated in terms of the geometric response function and penetration response function (GPRF). An approximate numerical method was proposed to implement the geometric and penetration response correction (GPRC) for keel-edge pinhole SPECT image reconstruction. A lookup table for the GPRC was calculated and then was utilized in the 3D pinhole iterative OSEM reconstruction procedure. The performance of the image reconstruction with the GPRC was evaluated using both the phantom and small-animal experiments in our micro-SPECT system. The results demonstrated significant improvements in the reconstructed image quality and resolution recovery. In conclusion, our approach using the GPRC method to the resolution recovery for the pinhole SPECT imaging is effective.

Index Terms—Pinhole SPECT, Keel-edge pinhole collimator, GPRC, image reconstruction

I. INTRODUCTION

To minimize the gamma-ray's penetration effect, pinhole collimator with keel-edge aperture has been widely utilized for high-resolution pinhole SPECT imaging. Although the keel-edge pinhole aperture could largely reduce the gamma-ray's penetration effect, it also causes significantly asymmetric geometric response and spatially variant geometric efficiency, which could result in distance-dependent and angle-dependent shift-variant resolution. So the compensation for the pinhole collimator response is of great importance in improving image quality and resolution recovery for high-resolution pinhole SPECT imaging.

The geometric response function (GRF) or geometric transfer function of collimator with channel aperture has been extensively studied by [1-5]. Those works are about the averaging GRF of moving collimator. For keel-edge pinhole collimator the GRF is varied significantly with the angle and

distance from the aperture and is a position-dependent function, so the averaging method to calculate GRF is not accurate in the present case. The geometric efficiency (GE) for keel-edge pinhole aperture was proposed and the corresponding compensation was also developed in Dr. Wang's Ph.D dissertation [6]. However, it was not presented how to calculate GRF in each detector bin and had not included the penetration effect, yet. In this study, we focus on the implementation of a 3D pinhole iterative image reconstruction method that includes both the geometric and penetration response corrections (GPRC) for keel-edge pinhole SPECT imaging. The derivations of geometric response and penetration response of keel-edge pinhole collimator were presented first. Then the implementation of the GPRC was discussed. The performance of image reconstruction with the GPRC was evaluated with experiment studies both using an Ultra-Micro Hot-Spot phantom and small animal imaging in our Micro-SPECT system.

II. METHODS

A. Geometric Response Function of Keel-edge Aperture

The Geometric Response Function (GRF) is defined as the distribution of detected photons emitted from a point source directly passing through the collimator aperture without penetration and scattering in the collimator material. It is often described as the probability density when the activity of a point source is normalized into unit intensity [5-7].

Since the source emits photons around with equal probability, the GRF could be derived from the detected solid angle divided by 4π steradians. If there is no collimator between the source and the detector, the GRF is derived to the equation (1) when adopting the Cartesian coordinate system. Where (x_f, y_f, z_f) and (x_d, y_d, z_d) are respectively the position coordinate of point source and the detected position in the detector plane, and ds is the area element in the detector. It could describe the distribution of GRF and the probability of a photon detected in the position ds at the detector.

$$GRF = \frac{(x_f - x_d)ds}{4\pi[(x_f - x_d)^2 + (y_f - y_d)^2 + (z_f - z_d)^2]^{\frac{3}{2}}} \quad (1)$$

The 3D profile of the GRF about non-collimated point source could be depicted in Fig.1. This figure illustrates the density distribution of GRF in which a source point with unit intensity was located 125 mm above the detector, and the magnitude of GRF is 10^{-6} at the heart region of the detector in this imaging situation.

Manuscript received November 10, 2008. This work was supported in part by the Chinese Nature Science Foundation under Grant number 30570520 and the Shanghai Pujiang Program.

Xuezhu Zhang is with the Graduate University of Chinese Academy of Sciences & Shanghai Institute of Applied Physics, Chinese Academy of Sciences, Shanghai 201800, China (telephone: +86-21-59557430, e-mail: zxz@sinap.ac.cn).

Qiusheng Dai is with the Graduate University of Chinese Academy of Sciences & the Shanghai Institute of Applied Physics, Chinese Academy of Sciences, Shanghai 201800, China (telephone: +86-21-59557430, e-mail: daiqsh@163.com).

Yujin Qi is with the Shanghai Institute of Applied Physics, Chinese Academy of Sciences, Shanghai 201800, China (telephone: +86-21-59554664, e-mail: yujinqi@yahoo.com).

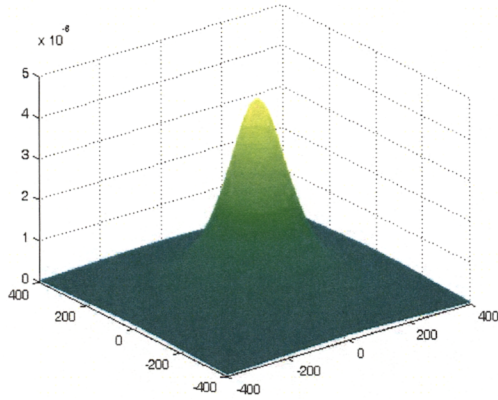


Fig.1 The illustration of the geometric point response function about the distribution of detected probability density on a detector from a non-collimated point source with unit intensity. The point source is located 125 mm above the detector. The magnitude of GRF is 10^{-6} at the heart region of the detector in this imaging situation

Now considering a collimator is equipped to the detector, the GRF is only a portion of direct passing through the keel-edge aperture in the above derived GRF. When a point source is placed off the central axis of the pinhole, the GRF is asymmetric and may cover different detector bins. The geometric efficiency (GE) of the point to the detector could be derived to equation (2) in which s represents the area of the geometric overlap.

$$GE = \frac{1}{4\pi} \iint_s \frac{(x_f - x_d) dy dz}{[(x_f - x_d)^2 + (y_f - y_d)^2 + (z_f - z_d)^2]^{\frac{3}{2}}} \quad (2)$$

Due to the channel height of the keel-edge pinhole, it is easy to prove that the direct geometric point response component is the overlap of two circles which the rays pass through the edge of the front aperture and the back aperture respectively. Fig.2 (a) shows the geometric response of the keel-edge pinhole collimator. Since the overlap is asymmetric and may cover different detector bins, we should consider its respective geometric response to each projection bin. Because

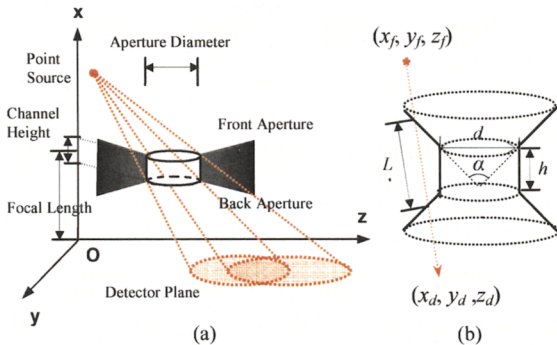


Fig.2 (a) The schematic of the geometric point response in the keel-edge pinhole collimator. The overlap of the two circles is the direct geometric component of the pinhole collimator response. (b) The schematic of the penetrative ray which passes through the keel-edge pinhole collimator.

the above integral operation in each detector bin is computation complexity, we will introduce an approximate analytical method to calculate the responses in subsection C.

B. Penetration Response Function of Keel-edge Aperture

The penetration response function of the keel-edge pinhole aperture was derived using an equivalent attenuation-length approximation method, which is illustrated in Fig.2 (b). It is different from the derivation about the penetration response of the knife-edge aperture which has been studied in [8-9]. The penetration length (L) of each gamma-ray was calculated by the distance of two points which are the intersections of the ray with the collimator surface. The derived equation (3) describes the point of intersection of penetrative ray from the keel-edge aperture, which includes the front conical surface (top), the cylindrical channel aperture surface (middle), and the back conical surface (bottom).

$$(y_a - y_p)^2 + (z_a - z_p)^2 = \begin{cases} \left[\tan\left(\frac{\alpha}{2}\right) \cdot (x_a - x_p) + \left(\frac{d}{2}\right) \right]^2 & \text{Top surface} \\ \left(\frac{d}{2}\right)^2 & \text{Middle surface} \\ \left[\tan\left(\frac{\alpha}{2}\right) \cdot (x_p - x_a) + \left(\frac{d}{2}\right) \right]^2 & \text{Bottom surface} \end{cases} \quad (3)$$

The known attenuation coefficient of the collimator material was used to calculate the attenuation-length terms [equation (4)]. The GRF_{pene} represents the penetrative geometric component passing through the collimator, which is derived from equation (1).

$$PRF = GRF_{pene} \cdot e^{-\mu L} \quad (4)$$

C. Approximate Method in the Implementation

The geometric and penetration response function (GPRF) on the detector could be calculated by the addition of GRF and PRF. Because of the magnification of the pinhole, the projection of one point source may cover different detector bins. Fig.3 (a) shows the asymmetric direct geometric component and the covered bins lying in the overlap of two circles.

If we use numerical integral method to calculate the GPRF of each detector bin, it will be a large computational work. We propose an approximate method to calculate the responses of each detector bin lying in the overlap and neighboring areas. The idea is that we partition each bin into n^2 grids. For example, in Fig.3 (b) we divide one bin into 64 grids. The area element ds is approximately substituted by the area of one grid. The center coordinate of each grid is used to calculate the approximate GPRF in that grid. Then the integration of calculating the responses of one bin is converted to sum the responses of all grids in that bin.

We developed a dedicated voxel-driven 3D pinhole OS-EM algorithm for the GPRC of keel-edge pinhole collimator. For the image experiments we need to calibrate the geometric system misalignment to ensure the reconstruction under a correct system coordinate for the GPRC. Then we could

calculate the lookup table (LUT) about the GPRF and incorporate the responses to the projection/ back-projection operation in the iterative image reconstruction procedure.

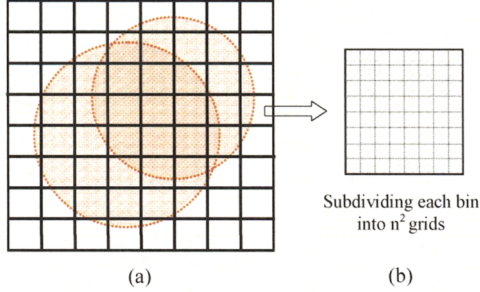


Fig.3 (a) The illustration of the geometric point response for the keel-edge pinhole. Due to the magnification of the pinhole, the overlap may cover different detector bins. (b) Subdividing one bin into n^2 grids to calculate the approximate GPRF in each detector bin.

III. EXPERIMENTS AND RESULTS

A. Comparison between Analytical Method and Monte Carlo Simulation

To validate the numerical method about GPRF which we have presented in section II, we made a comparison study between our analytical method and the Monte Carlo simulation. The system used in the simulation was based on a micro-SPECT system which was developed in our lab [10-11]. The detector is a pixellated NaI(Tl) crystal array with 1.4 mm pixel pitch and 5 mm thickness coupled to a 5" Hamamatsu R3292 PSPMT. The pinhole collimators were made of tungsten alloy with different sizes of keel-edge aperture, and the open angle is 60° . The aperture size ranges from 2.0 mm to 0.65 mm, but the channel height of these pinhole collimators is identical to 0.5 mm. The focal length is 100 mm which could result in a magnification of $2 \sim 3.3$ for the routine experiments.

We used the MCNP package to simulate the point source response function of pinhole collimator. The scattering in the collimator and crystal material was considered in MC simulation. A large number of photon histories ($\sim 5 \times 10^8$) were used to provide a noise-free image. The simulated gamma energy is 140keV. The point source was simulated at a position of 25mm from the pinhole aperture with 20 degree oblique from the central axis of the pinhole collimator. The simulated aperture size is 1.0mm and the channel height is 0.5mm. The analytical geometric response and penetration response functions of the point source were also calculated in the same imaging condition.

Fig.4 shows the comparison results between the Monte Carlo simulation and the analytical method for calculating the geometric point response (left) and penetration point response (right) of a single keel-edge pinhole collimator which is equipped to the midpoint of the detector. The figures in (a) and (b) are the results of analytical calculation results. The figures in (c) and (d) are the results of MC simulation. The

results show that the analytical method could provide almost the same GRF and PRF as the MC method.

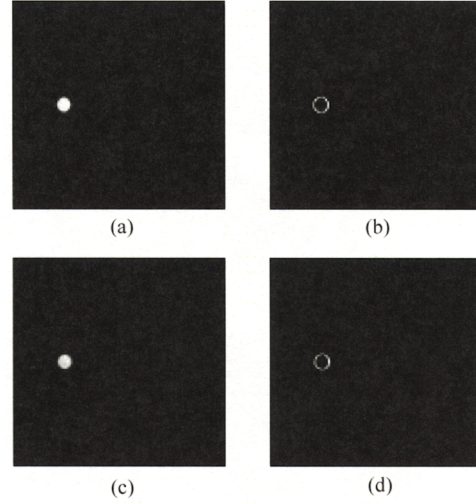


Fig.4 The comparison between the analytical method and the Monte Carlo simulation for calculating the geometric point response (left) and penetration point response (right) of a single keel-edge pinhole collimator. The simulated aperture size is 1.0 mm and the channel height is 0.5 mm. The point source was simulated 25 mm above the pinhole with 20 degree oblique from the central-axis of the keel-edge aperture. The (a) and (b) are analytical calculation results. The (c) and (d) are MC simulation results.

B. Phantom SPECT Imaging Experiment

To evaluate the performance of this compensation method, we performed an experimental study using an Ultra-Micro Hot Spot phantom (Data Spectrum Inc.) filled with $\sim 5\text{mCi } ^{99\text{m}}\text{Tc}$ pertechnetate in the water solution. The experiment was performed in our micro-SPECT system using keel-edge pinhole collimator with 4 different diameters of 2.0, 1.5, 1.0, and 0.65 mm respectively. The projection data for each pinhole aperture were acquired with 90 angular views equally spaced over 360° , and the acquisition time was 30 seconds per view. The radius-of-rotation (ROR) was ~ 35 mm, which results a magnification of ~ 3 . The projection data were reconstructed using a voxel-driven 3D pinhole OS-EM algorithm without any correction and with GPRC. The OS-EM image reconstructions took 9 subsets and 5 iterations. The post-filtering was used for the results of reconstruction images. The reconstructed transaxial images of the Ultra-Micro Hot Spot phantom were shown in Fig.5. As compared to the conventional OS-EM algorithm without any correction, the GPRC shows consistently improvements in the image resolution and the overall quality with the pinhole apertures varying from 2.0 mm to 0.65 mm, and the system resolution is significantly improved to well resolve the 0.75 mm rods using the 0.65 mm pinhole aperture.

C. Small animal SPECT Imaging Experiment

The GPRC method was further evaluated by in vivo small-animal imaging experiment. The bone-scan imaging of a

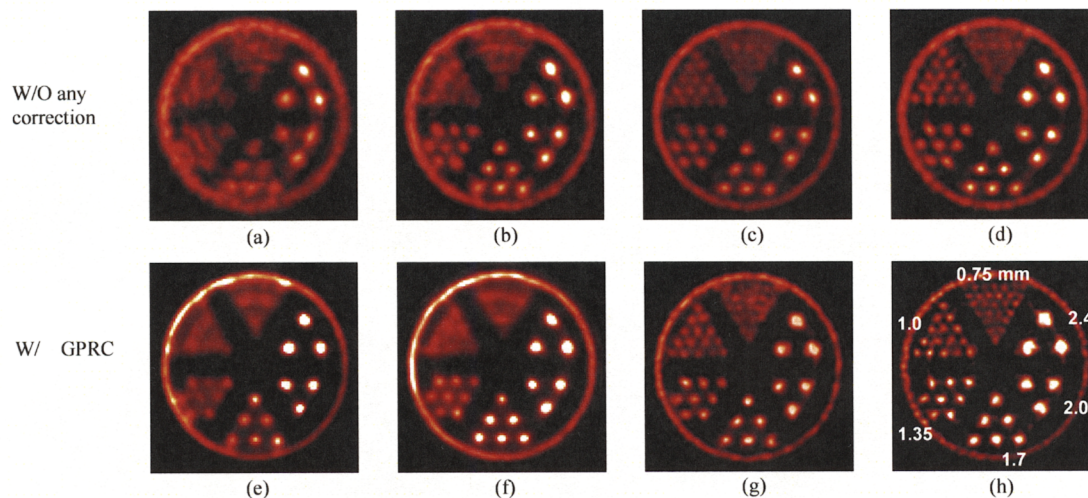


Fig.5 The comparison of the reconstructed images of Ultra-Micro Hot-Spot phantom using voxel-driven 3D keel-edge pinhole OS-EM algorithm between the reconstruction without any correction (top row) and with the GPRC (bottom row). The figures from left to right show the results of different aperture sizes representing 2.0 mm (a), 1.5 mm (b), 1.0 mm (c), 0.65 mm (d) (h). All these reconstructed images are smoothed by the post-filtering.

~30g normal mouse injected with ~5mCi ^{99m}Tc -MDP was performed around the mouse's chest. The projection data were acquired with 90 views over 360° and 30 seconds per view using a 0.65 mm keel-edge pinhole aperture. The images were reconstructed using a 3D pinhole OS-EM algorithm with the GPRC correction, shown in Fig.6. The details of mouse's bone structure, such as the vertebra and ribs, are clearly resolved out.

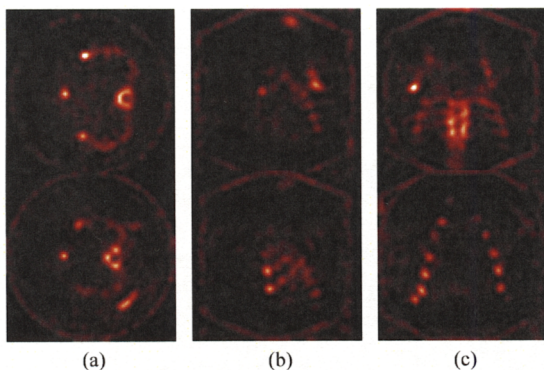


Fig.6 The OS-EM reconstruction results of 3D keel-edge pinhole GPRC for a mouse bone SPECT performed around the mouse's chest with ^{99m}Tc -MDP. The figures from left to right show the selected slice of (a) transaxial, (b) sagittal, and (c) coronal reconstruction image

IV. SUMMARY AND CONCLUSION

We have analytically derived the geometric and penetration response function of the keel-edge pinhole collimator. An approximate analytical method has been proposed to calculate the GPRF in each detector bin. A LUT for the GPRC was calculated and then utilized in the projection/back-projection operation of the OS-EM iterative reconstruction algorithm

study. The performance of the image reconstruction with the GPRC was evaluated using both the Ultra-Micro Hot Spot phantom and small animal SPECT imaging experiment in our micro-SPECT system. The results from the phantom imaging study show that the pinhole image reconstruction which includes the GPRC has significantly improved the image quality, image resolution and quantitative accuracy as compared to the conventional pinhole OS-EM reconstruction without any correction. In conclusion, our approach about the GPRC to the resolution recovery for the pinhole SPECT imaging is effective and reliable.

REFERENCES

- [1] C. E. Metz, F. B. Atkins, and R. N. Beck, "The geometric transfer function component for scintillation camera collimators with straight parallel holes", *Phys.Med.Biol.*, Vol. 25, No. 6, pp. 1059-1070, 1980.
- [2] B. M. W. Tsui and G. T. Gullberg, "The geometric transfer function for cone and fan beam collimators," *Phys.Med.Biol.*, Vol. 35, No. 1, pp. 81-93, 1990.
- [3] G. L. Zeng, and G. T. Gullberg, "Three-dimensional iterative reconstruction algorithms with attenuation and geometric point response correction," *IEEE Trans. Nucl. Sci.*, Vol. 38, No.2, pp.693-702, June, 1991.
- [4] I. Laurette, G. L. Zeng, A. Welch, P. E. Christian and G. T. Gullberg, "A three-dimensional ray-driven attenuation, scatter and geometric response correction technique for SPECT in inhomogeneous media," *Phys. Med. Biol.*, Vol. 45, pp. 3459-3480, 2000.
- [5] E.C.Frey, B.M.W.Tsui, G.T.Gullberg, "Improved estimation of the detector function for converging beam collimator," *Phys. Med. Biol.*, Vol. 43, pp.941-950, 1998.
- [6] Yuchuan Wang, "Development and application of high-sensitivity and high-resolution fully 3D SPECT imaging techniques using two different collimator designs," *Ph.D. dissertation*, The University of North Carolina at Chapel Hill, 2004.
- [7] V. Bekaert, D. Brasse, B. Gizard, and J.-L. Guyonnet, "Determination of the analytical point spread function of a pinhole aperture SPECT system," in *Conf. Rec. IEEE Nuclear Science Symp.*, 2004, pp. 2565-2569

- [8] M. F. Smith and R. J. Jaszcak, "An analytic model of pinhole aperture penetration for 3D pinhole SPECT image reconstruction", *Phys.Med.Biol.*, Vol.43, pp. 761-775, 1998.
- [9] S. D. Metzler, J. E. Bowsher, M. F. Smith and R. J. Jaszcak, "Analytic determination of pinhole collimator sensitivity with penetration," *IEEE Trans. Med. Img.*, Vol. 20, pp.730 -741, 2001.
- [10] Yujin Qi, "Optimized Collimator Designs for Small Animal SPECT Imaging With a Compact Gamma Camera," in *IEEE EMBS Conf.*, 2005, pp. 1780-1782.
- [11] Y.J.Qi, M.J.Zhang, C.L.Zhao and R.F.Wojcik, "Performance Comparison of Subtractive resistive readout with conventional resistive readout for high-resolution compact gamma camera," in *Conf. Rec. IEEE Nuclear Science Symp.*, 2007, pp. 3725-3728.